J Appl Electrochem (2015) 45:1–10
DOI 10.1007/s10800-014-0754-3

RESEARCH ARTICLE

Towards the realistic silicon/carbon composite for Li-ion secondary battery anode

Krzysztof Kierzek · Jacek Machnikowski · François Béguin

Received: 26 June 2014 / Accepted: 22 September 2014 / Published online: 1 October 2014

Abstract A practical and inexpensive method for producing Si/C composite as ready-to-use active material for Li-ion battery anode has been developed. Three-component powders (<63 μm) were synthesized by embedding micro-sized silicon (8–24 wt%) and synthetic battery-grade graphite (60–75 wt%) in a pitch-derived carbon matrix. The procedure consisted of short mechanical milling of silicon with toluene/pitch suspension followed by mixing with graphite and final heat-treatment at 1,100 °C. X-ray diffraction was applied for determining the structural characteristics of the composite and impurities present. A series of anodes were prepared by using CMC and PVDF binder. The dispersion of silicon particles in the carbon matrix and spreading of the binder into the anodic film were monitored using the SEM–EDX technique. Lithium insertion/deinsertion performance was assessed from the galvanostatic charge–discharge characteristics using a Si/C–lithium two-electrode cell. Embedding silicon in well conductive pitch coke as well as reducing the content of carbon black as percolator allowed the first cycle irreversible capacity to be decreased to 90 mAh g^{-1}. An initial reversible capacity of 620 mAh g^{-1} for 12 wt% of Si in the composite, with average capacity decay of 0.3 % per cycle, was achieved thanks to a specific composite structure as well as profitable physicochemical properties of the CMC binder. Intensive press-rolling of the anodic film allowed the packing density to be increased up to 1.35 g cm^{-3} (9.5 mg cm^{-2} at thickness of 70 μm) and, as a result, an outstanding volumetric capacity up to 670 mAh cm^{-3} could be achieved, without changing the cycling properties.

Keywords Silicon/carbon composites · Lithium batteries · Cycle life · Calendering · CMC binder

1 Introduction

The recent increased production of portable electronic devices, i.e. mobile phones, tablets, and notebooks, has created a greater demand for high-performance, lightweight, and compact electric power sources. Currently, the Li-ion batteries seem to be the best energy storage system for such applications. Due to strong competition among battery manufacturers, the capacity of the typical cell grows, approximately, by 10 % annually [1], and today's high-end industrial 18650-type cylindrical batteries show unit capacities above 3 Ah (e.g. Panasonic NCR18650B). The increase in energy density is related to elimination of void cell space as well as improving the electrode material performance [2].

The materials generally used in the industrial Li-ion batteries are lithium transition metal oxides for the cathode and graphite for the anode. The specific capacity of commercial cathodic materials is 140–170 mAh g^{-1} with possibility of further improvement. The theoretical graphite capacity is 372 mAh g^{-1}, but the real charge accumulation depends strongly on the precursor materials and synthesis conditions and rarely exceeds 360 mAh g^{-1} at low current load. The capacity of 362 mAh g^{-1} which is reported for the massive artificial graphite developed by Hitachi

K. Kierzek (✉) · J. Machnikowski
Department of Polymer and Carbonaceous Materials, Faculty of Chemistry, Wroclaw University of Technology, Gdanska 7/9, 50-344 Wroclaw, Poland
e-mail: krzysztof.kierzek@pwr.edu.pl

F. Béguin
Institute of Chemistry and Technical Electrochemistry, Poznan University of Technology, Piotrowo 3, 60-965 Poznan, Poland

Chemical Co. Ltd. seems to be a limit for graphite-like anodic materials [3]. Some disordered carbons demonstrate a higher reversible capacity than graphite (about 500 mAh g^{-1}), but with several serious drawbacks. An enhanced irreversible capacity and wide hysteresis between charge and discharge occur in this kind of material [4]. Moreover, an important part of discharge is close to 0 V versus Li/Li^+, increasing the risks of lithium plating during fast charging of the battery. To keep abreast of continuous progress in the cathodic material performance, new higher charge capacity materials should substitute graphite in the negative electrode in the future [5].

There are several metals which can be electrochemically alloyed with Li. The most promising are silicon and tin of theoretical capacity around 4,200 and 990 mAh g^{-1}, respectively [6]. However, the application of a pure metal as anodic material is problematic because of a huge swelling (up to 300 % in case of Si) and a poor reversibility of lithium storage. Nevertheless, battery companies have already shown a prototype cell containing these metals. Amprius Inc. demonstrated that lithium can be reversibly stored in an anode built of silicon nanorods or nanotubes with metallic filaments fixed laterally to the current collector [7]. The specific morphology and nanostructure of silicon allowed to achieve a very high charge capacity without mechanical disintegration. The first prototype cell was demonstrated in 2008, however, no consumer product had been presented on the market until now. It is probably due to difficulties in scaling-up the complicated silicon growing process. Another concept is forced by Sony Corporation. The company promotes the new Li-ion battery line named Nexelion, where a Sn/Co/C composite anode is used as lithium host [8]. The Nexelion cell demonstrates a very high initial capacity (3.5 Ah in 18650 size) and quick charge capability (up to 90 % in 0.5 h), but the cycle life of the system is still unsatisfactory (9 % of capacity decay after 100 cycles [9]) in relation to the conventional graphite-based cell.

The substitution of graphite by a Si/C or Sn/C composite seems to be the most realistic concept of an advanced anode on account of cheap raw materials and potentially easy to scale-up production process. Silicon is the most widely studied active material of such composites [10–15]. Generally, all the reported protocols of composite preparation include the reduction of silicon particle size and their homogenous embedding in a carbon matrix. Small silicon particles exhibit low absolute swelling amplitude. The role of the matrix is to accommodate the silicon expansion and to assure the electrode conductivity on a reasonable level to facilitate the charge transfer to the hosts. For that reason, a well-ordered carbon should be preferred as a matrix material [14, 16–18].

As reducing the swelling amplitude of Si particles is crucial for the composite performance, nanopowder of particle size below 100 nm has been the most often used until now. However, nanosilicon has a tendency to make aggregates of size around 1 μm, and very thorough homogenization is required to maintain its dispersion in the carbon matrix [17]. Other drawbacks are the price and the limited supply of Si nanopowder, caused by a complicated manufacturing process (laser ablation). Therefore, it is surprising that some authors claim the composite based on nanosilicon to be a "cheap" anode material [18].

Recent studies show that the performance of Si-based anodes also strongly depends on the content of percolator (mostly carbon black) and the kind of polymeric binder applied [18–21]. The carboxylic groups occurring in some polymers, such as the carboxymethyl cellulose (Na-CMC) sodium salt and polyacrylic acid (PAA) can interact with functionalities occurring on both carbon and silicon surfaces to create a beneficial hybrid network [22]. In addition, the specific porous texture created can accommodate the textural stresses during cycling. In consequence, a huge improvement of capacity retention is observed [19]. The poor electric conductivity of the binder can be compensated by increasing the percolator content. Since very often anodes with more than 20 wt% of carbon black are fabricated [18, 19], the main drawback of such composition is a significant reduction of electrode density and, finally, volumetric capacity. Moreover, the irreversible capacity undesirably grows due to a higher surface area exposed to the electrolyte. Actually, the priority of portable electronics manufactures is to decrease the size of battery rather than its weight. Therefore, reducing the content of binder and percolator to achieve a high volumetric energy density of anode is recommended. Notwithstanding, the specific density of the Si-based anode is rather rarely reported, and consequently, a comparison with a conventional graphite-based cell is not possible.

Within this context, the objective of this work is to develop a facile and ready to scaling-up synthesis method of Si/C composite suitable as active material of anode in Li-ion battery. The composite consists of silicon and graphite microparticles embedded in a pitch coke matrix. Only cheap and easily available raw materials were used in the synthesis, and the amount of binder and conductive additive applied for the anode fabrication was kept at a reasonably low level. The gravimetric as well as volumetric capacities of the Si-based anode were assessed and compared to those reported for the conventional graphite electrode.

2 Experimental section

2.1 Si/C composite preparation

The raw materials used for Si/C composite preparation were silicon powder (Aldrich) with a particle size below

78 μm (325 mesh), synthetic battery-grade graphite powder (TIMREX® SLP30, Timcal), and coal-tar derived pitch. Silicon is the main active component of the composite, and the role of graphite is to increase the intrinsic conductivity of the final Si/C particles while contributing partly to the overall capacity. A special particulate matter-free pitch of softening point 97 °C (Mettler) and low heteroatom content was selected to produce a soft-carbon matrix with a moderate irreversible capacity.

The protocol which was applied to obtain a homogeneous composite consisted of the following steps. Firstly, the slurry of pitch and silicon in toluene was ground for 2 h by ball milling (SPEX CertiPrep 8000M) using tungsten carbide balls (diameter of 4 mm) and vial. The mass ratio of balls to silicon and pitch was 5:1. Toluene kept the mixture liquid and helped to transport heat to the vial walls. The high molecular weight pitch constituents dispersed in toluene during milling like a protective colloid and inhibited the agglomeration of silicon particles or the undesirable cold welding process [23, 24]. Next, graphite powder was added to the slurry, and the mixture was heated-up to 520 °C stirred in a glass retort under nitrogen and soaked for 2 h to distil-off the solvent and to pyrolyse the pitch binder. The resultant material was ground to a particle size below 63 μm. A final heat-treatment was performed under nitrogen in a horizontal quartz reactor at 1,100 °C by soaking for 3 h. Composites with similar pitch coke contribution of about 17 wt%, 8–24 wt% of silicon, 59–75 wt% of graphite were prepared according to the described protocol. The composition of the composites was determined on the basis of the residue yield of pure pitch carbonized and an assumption that the mass of silicon and graphite did not change. The composites were named xxSi/C where "xx" represents the silicon weight percent. For comparison, a material labeled F-12Si/C with unmodified silicon particle size was prepared by omitting the ball milling step. The detailed composition of all prepared materials is shown in Table 1.

2.2 Electrode preparation and electrochemical measurements

A series of electrodes was prepared with 80 wt% Si/C composite, 5 wt% carbon black of a high aggregation degree (C-NERGY™ SUPER C65, Timcal), 12 wt% Na-CMC (Aldrich, MW ~700,000), and 3 wt% styrene-butadiene rubber SBR (MTI Corp., USA) using the following protocol. A slurry obtained by mixing the Si/C composite and carbon black with a water suspension of CMC/SBR and small amount of non-ionic surfactant (Tween 20, Aldrich) was cast on battery-grade copper foil (Schlenk, Germany, 25 μm) used as current collector. The solvent was evaporated at 120 °C under vacuum overnight, and then the film was press-rolled under different forces. Calendering was performed to 100 % (not pressed), 60, 40, and 30 % of the initial film thickness, which was set individually so that all final electrodes had the similar thickness in the range of 60–70 μm excluding the current collector. Electrodes with a diameter of 15 mm were punched out, dried under vacuum at 120 °C overnight to remove traces of water and surfactant and, finally, introduced in an argon filled glove-box. The resultant electrodes were marked with extension "-CMC-yy" where "yy" represents the press-rolling intensity (e.g. "-CMC-60" means that an electrode was calendered to 60 % of the initial film thickness).

In the case of the electrode with polyvinylidene difluoride (PVDF) binder, *N*-methylpyrrolidone was used as solvent. The film consisting of 85 wt% of composite 12 wt% Si, 5 wt% carbon black, and 10 wt% PVDF (Solef 5130, Solvay) was press-rolled to the level of 60 %. The final electrode was named 12Si/C-PVDF-60.

Electrochemical testing was performed in coin-type cells (CR2032, Hohsen Corp., Japan), which were assembled with the Si/C-based electrode as anode and a metallic lithium foil as cathode and reference electrode. The electrolyte used was a 1 M solution of lithium hexafluorophosphate ($LiPF_6$) in a 1:1 (v/v) mixture of EC (ethylene carbonate) and DMC (dimethyl carbonate). A glass microfiber separator (Whatman, GF/F, thickness of 420 μm), wetted with the electrolyte, was sandwiched between the carbon electrode and the Li metal foil.

The cells were investigated by galvanostatic cycling using a VMP3 (Biologic, France) multichannel generator. The charging/discharging rate was set at C/5, i.e. corresponding to the theoretical capacity of graphite (372 mAh g^{-1}) in 5 h, in a potential range from 0.005 to 1.5 V versus Li/Li^+. The galvanostatic characteristics of the cells were used to determine the reversible capacity (C_{rev}), irreversible capacity (C_{irr}), and the coulombic efficiency (CE) defined as the ratio of deinsertion to insertion charge expressed in percent. The charge capacity was related to the mass of Si/C composite in the anode or to the total mass of anodic film (including the binder and carbon black).

2.3 Structural and textural characteristics

X-ray diffraction was used for the structural characterization of the Si/C composites. The measurements were

Table 1 Contribution of silicon, graphite, and pitch-derived coke in the composites prepared

Composite	Si (wt%)	Graphite (wt%)	Coke (wt%)
8Si/C	8	75	17
12Si/C	12	71	17
18Si/C	18	65	17
24Si/C	24	59	17
F-12Si/C	12	71	17

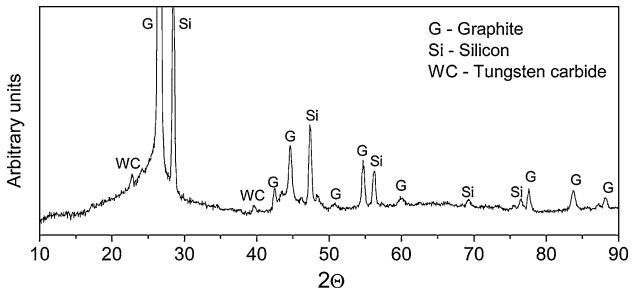

Fig. 1 X-ray diffraction pattern of the 12Si/C powder

performed on a Rigaku powder diffractometer ULTIMA IV at 40 kV accelerating voltage using the CuKα radiation of wavelength $\lambda = 0.15406$ nm. The morphology and homogeneity of the anodes were assessed by scanning electron microscopy (Zeiss EVO LS15) coupled with energy dispersive X-ray analysis (EDX, Bruker Quantac 200).

The calendered anodic mass which was collected by mechanical detaching of the film from the current collector was characterized in terms of porosity development. The micro- and mesoporous texture (0.6–50 nm width) was characterized by nitrogen adsorption at 77 K in the p/p_0 range from 10^{-7} to 0.98 (ASAP 2020, Micromeritics). The N_2 adsorption data were used to determine the BET specific surface area S_{BET}, the total pore volume V_T, and the micropore volume V_{DR} [23]. CO_2 adsorption at 273 K was used (NOVA 2200 Quantachrome) to characterize the ultramicropore (<0.7 nm) volume (V_{DR,CO_2}) and the specific surface area (S_0) by the application of the Dubinin–Radushkevich [25] and Stoeckli [26] equations to the adsorption data in the pressure range of 2 Pa–20 kPa. Mercury porosimetry up to 414 MPa (Autopore IV, Micromeritics) was applied to analyze pores with width in the range of 3.6 nm–15 µm.

3 Results and discussion

3.1 Characterization of materials

The X-ray diffraction pattern of the Si/C composites is typical of a simple physical mixture of components: pitch coke, silicon, and graphite (Fig. 1). There is no evidence either of silicon and graphite amorphization during milling or of silicon carbide formation on heat-treatment. Only weak signals from traces of inorganic impurities from ball milling are recorded, e.g., tungsten carbide.

The morphology of the electrodes with CMC and PVDF binders is presented in Figs. 2a and 3a, respectively. All the electrode components (Si/C composite, binder, and percolator) can be easily recognized on the images. The original "potato shape" of the SLP30 graphite particles has not been changed. A different dispersion of the two polymers should be noticed. Na mapping reveals that the CMC binder is very well dispersed on the Si/C particles surface (Fig. 2d). In contrast, F mapping indicates that PVDF has a tendency to form aggregates, and the composite particles are only partially coated by this binder (Fig. 3d).

Si mapping (Figs. 2c, 3c) suggests that the homogeneity of the Si/C composite is not perfect, and few bulk particles or aggregates are distinguished in the images as more brighter points. A part of silicon is not well embedded in the bulk of pitch coke and is presented as uncovered regions.

The increase in bulk density during calendering reflects the reduction of interparticle voids of the electrode, as demonstrated by the decrease of pore volume measured by mercury porosimetry (Fig. 4) from ~ 0.85 cm^3 g^{-1} in 12Si/C-CMC-100 to ~ 0.65 cm^3 g^{-1} in 12Si/C-CMC-30. The non-pressed electrode is characterized by an abundance of pores with diameter between 1 and 5 µm. Press-rolling of the anodic material to 30 % of the initial thickness results in a drastic decrease in pore volume in the range of 0.01–20 µm (about 2.6 times, Fig. 4b) and a shift of interparticle void size to lower values. The maximum in the wide pore diameter distribution is located at 0.3 µm.

The N_2 and CO_2 adsorption isotherms (Fig. 5) show that press-rolling influences the electrode micro- (<2 nm width) and mesoporosity (2–50 nm) opposite to macroporosity (>50 nm). The increase in adsorption capacity is most pronounced in the high p/p_0 region of Fig. 5a, corresponding to the adsorption in large mesopores. The porous texture parameters calculated from the isotherms (Table 2) are higher, especially the total pore volume V_T, for 12Si/C-CMC-30 than for 12Si/C-CMC-100. Such a behavior can be attributed to the considerable reduction in size of interparticle voids which shift, in part, into the region measurable by gas adsorption.

The very small N_2 adsorption capacity in the low p/p_0 region and the overall CO_2 adsorption capacity evidence a very low contribution of narrow micropores in the electrodes. It can be considered as the effect of very little intraparticle porosity of the active constituents (silicon, graphite, and pitch coke), but also of the low carbon black content. The BET specific surface area is in the range of 2–4 m^2 g^{-1}, i.e. lower than that of TIMREX® SLP30 graphite (7 m^2 g^{-1}, according to Timcal datasheet).

3.2 Electrochemical properties

3.2.1 Role of binder

The galvanostatic curves of the first discharge/charge cycle of electrodes obtained from the composite with 12 wt% of

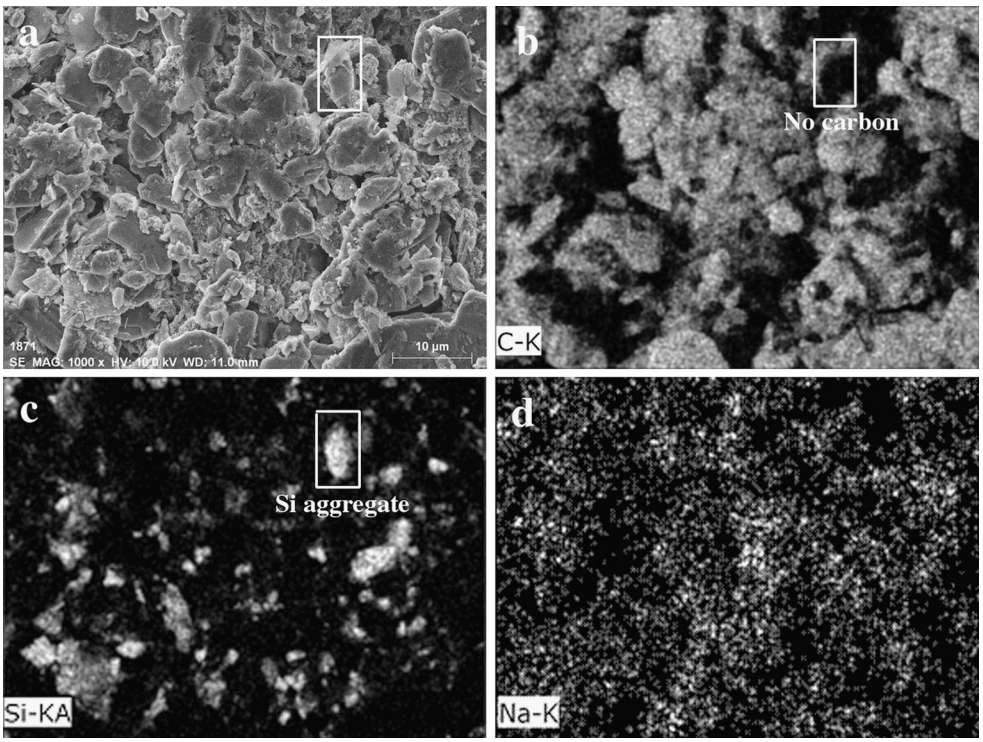

Fig. 2 SEM image (**a**) and X-ray elemental map of C (**b**), Si (**c**), and Na (**d**) of 12Si/C-CMC-60 anode

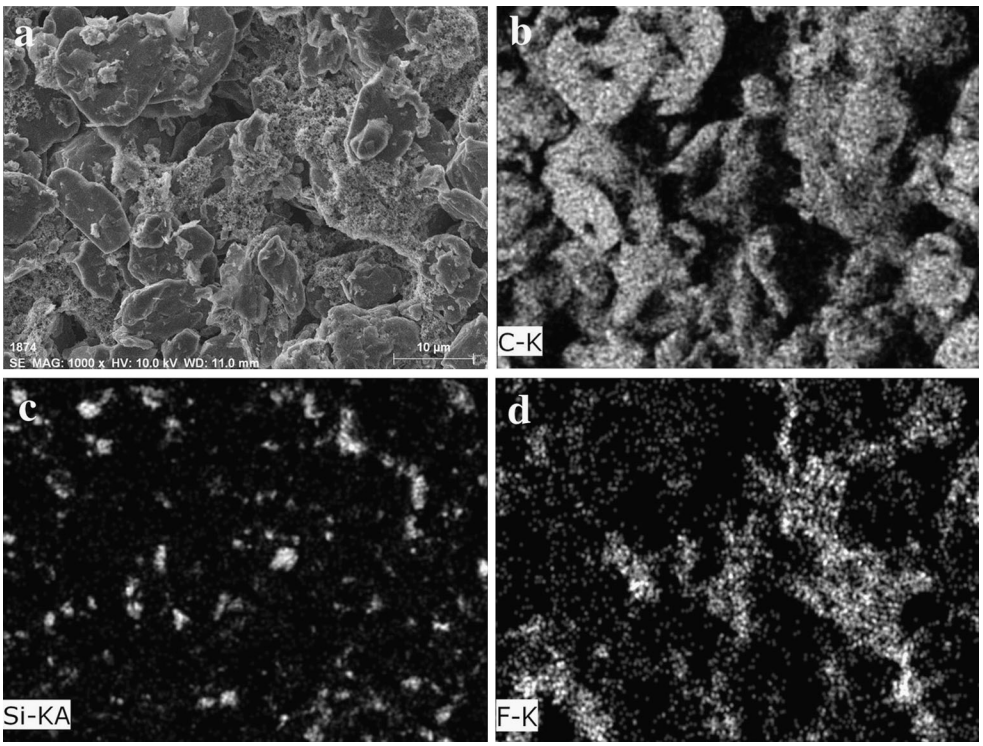

Fig. 3 SEM image (**a**) and X-ray elemental map of C (**b**), Si (**c**), and F (**d**) of 12Si/C-PVDF-60 anode

Si using Na-CMC and PVDF as binder are shown in Fig. 6. Characteristics of two anodes made by different method are also given for comparison: (a) anode made of a Si/C composite containing graphite, pitch coke, and silicon of unmodified particle size (ball milling step omitted; labeled F-12Si/C-CMC-60), (b) anode made of a mixture of ball

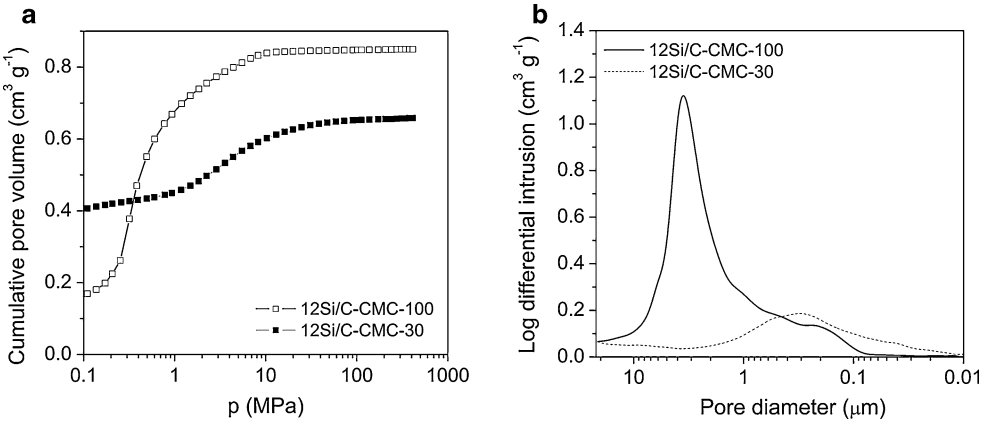

Fig. 4 Mercury intrusion (**a**) and pore size distribution (**b**) of the 12Si/C-CMC-100 and 12Si/C-CMC-30 anodic materials

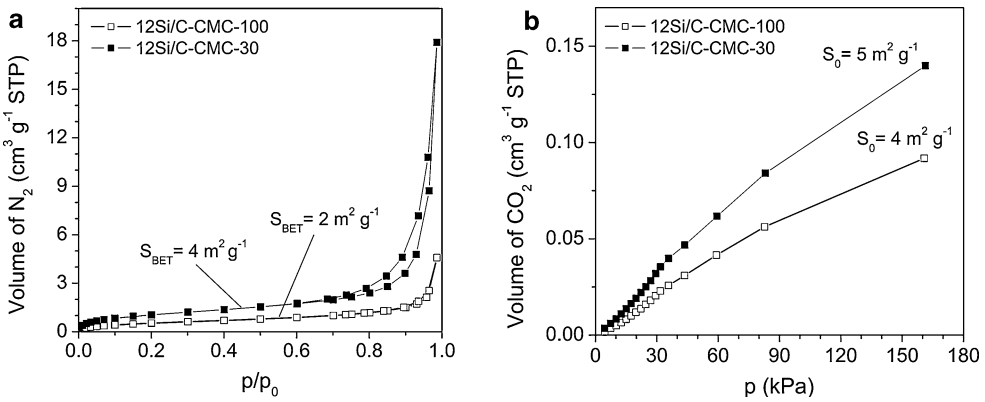

Fig. 5 N_2 (**a**) and CO_2 (**b**) adsorption/desorption isotherms of the 12Si/C-CMC-100 and 12Si/C-CMC-30 anodic materials

Table 2 Micro- and mesoporosity parameters of selected anodic materials

Anodic material	N_2 adsorption			CO_2 adsorption	
	S_{BET} (m^2 g^{-1})	V_{DR,N_2} (cm^3 g^{-1})	V_T (cm^3 g^{-1})	V_{DR,CO_2} (cm^3 g^{-1})	S_0 (m^2 g^{-1})
12Si/C-CMC-100	2.0	0.0007	0.0033	0.0021	4.0
12Si/C-CMC-30	3.9	0.0015	0.0130	0.0034	5.3

milled Si in toluene for 2 h (12 wt%) and graphite (88 wt%) with Na-CMC as binder (labeled R-12Si/C-CMC-60).

A large initial reversible capacity, above 600 mAh g^{-1}, was measured for all the electrodes with only a slight effect of the electrode preparation procedure (Fig. 6a). The distinct charge/discharge hysteresis is typical of Si-based anodes and is related with the electrochemical properties of this metal. An exceptionally low irreversible capacity, below 100 mAh g^{-1}, must be pointed out for the three materials. Such low C_{irr} is very rarely reported for Si/C composites of comparable reversible capacity. Usually C_{irr} values are from 180 to even 500 mAh g^{-1} [19, 20, 23, 27]. The improvement can be attributed to the low amount of active sites where the electrolyte irreversibly decomposes, forming the SEI layer, as well as limited lithium trapping in the silicon phase. Electrolyte decomposition was reduced mostly by lowering the content of carbon black and binder as well as other impurities, i.e. WC from ball milling. The low specific surface area of anodes (Table 2) well corresponds with the low C_{irr}.

The galvanostatic charge/discharge cycling (Fig. 6b) increases the differentiation of the electrodes. The reversible capacity of the PVDF-based anode drastically drops in 30 cycles down to 170 mAh g^{-1}. A similar behavior is shown by the anodes based on the Si/C composite containing silicon coarse powder (F-12Si/C-CMC-60) or built from the physical mixture of silicon fine powder and graphite with CMC binder (R-12Si/C-CMC-60). In all cases, the capacity loss is associated with a significant

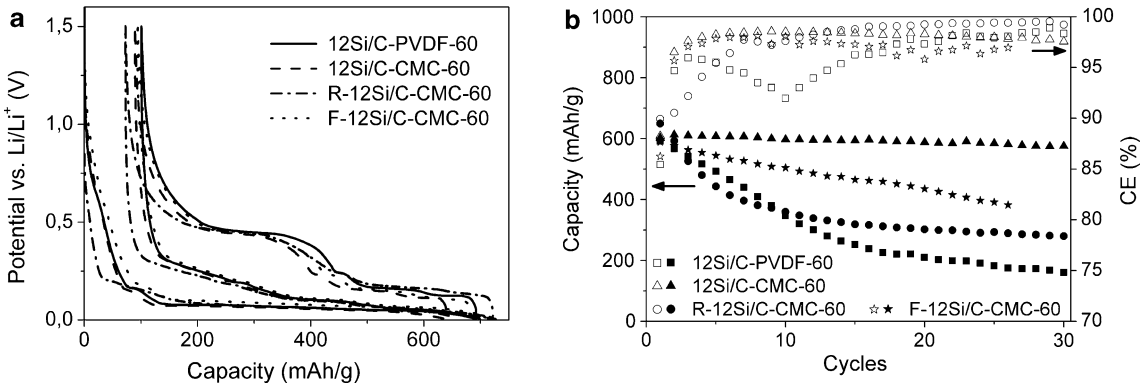

Fig. 6 Potential profiles of the first discharge/charge cycle (**a**) and cyclability (**b**) of Si/C-based anodes prepared from different procedures. The values are related to the mass of Si/C composite in the anode

decrease of the coulombic efficiently around the 10th cycle. Only embedding the very fine Si particles in the carbon matrix together with binding the final powder by CMC gives limited capacity decay, about 0.3 % per cycle. The improved performance of the anode seems to result from the specific composite structure and CMC binder properties. The pitch coke sufficiently accommodates the swelling of Si particles of limited size, like in 12Si/C, and the conductive carbon matrix facilitates the charge exchange between the silicon component and the current collector even after amorphization of silicon during the first delithiation [28, 30]. Bigger Si particles, like in the F-12Si/C material, exhibit higher swelling amplitude which cannot be accommodated by coke. Swelling of small amount of isolated Si particles can be easily accommodated by the CMC binder. Moreover, the homogenous and stiff network created by the CMC binder causes that the original current paths established by carbon black during press-rolling of the electrode are more stable during cycling than those created in PVDF, which noticeably swells in the electrolyte [29]. Consequently, the amount of lithium irreversibly trapped in silicon and graphite is significantly reduced when using the CMC binder.

3.2.2 *Effect of Si content in the composite*

Increasing the silicon content in the composite from 8 to 18 wt% enhances the C_{rev} of the first cycle without changing C_{irr} which is maintained below 100 mAh g^{-1} (Fig. 7a). The C_{irr} of the composite with 24 wt% of silicon is enlarged to 141 mAh g^{-1}. It clearly proves that the irreversible loss is induced by the SEI formation together with lithium trapping in the silicon phase. The carbon matrix capability for charge transfer to the pristine silicon phase is attenuated only above 18 wt% of Si. Unfortunately, cycling tests (Fig. 7b) suggest that the maximum Si content should not exceed about 12 wt%. After 50 charge/discharge cycles, the capacity of 12Si/C-CMC-60 amounts to 525 mAh g^{-1}, a value which is much higher than the one achieved with graphite at similar current load (340–350 mAh g^{-1}). Increasing the Si loading to 16 and 24 wt% results in fast capacity fading what is, probably, an effect of stronger mechanical disintegration of the anodes. After 50 cycles, the reversible capacity decreases to about 100 mAh g^{-1}.

3.2.3 *Effect of electrode packing density*

From the practical point of view, it is more important to enhance the anode volumetric capacity than the gravimetric one. It can be achieved by decreasing the content of electrochemically inactive components (binder, percolator etc.) or increasing the packing density. In this work, using the composite with 12 wt% of Si, we assessed the effect of force applied during electrodes press-rolling (calendering) on the density of the anodic film and on the values of gravimetric and volumetric capacities (Fig. 8). Calendering the anode mass up to 30 % of the initial film thickness appears to be possible without electrode damaging; the gravimetric capacity, related to the total anodic mass, remains at a level of about 500 mAh g^{-1}. The density increases exponentially with the force to reach 1.35 g cm^{-3} upon compacting to 30 % of the initial thickness. No further density increase was possible because of film detaching from the copper foil. An outstanding volumetric capacity of 670 mAh cm^{-3} was calculated for the 12Si/C-CMC-30 anode, based on the measured gravimetric capacity and density; this value is higher than that reported for the best commercial graphite-based anodes (about 610 mAh cm^{-3}) [31].

As shown in Fig. 9, the cycling performance of the anodes is almost unaffected by increasing the force during press-rolling of electrodes made from the 12Si/C composite. All anodes show similar and very high coulombic efficiency.

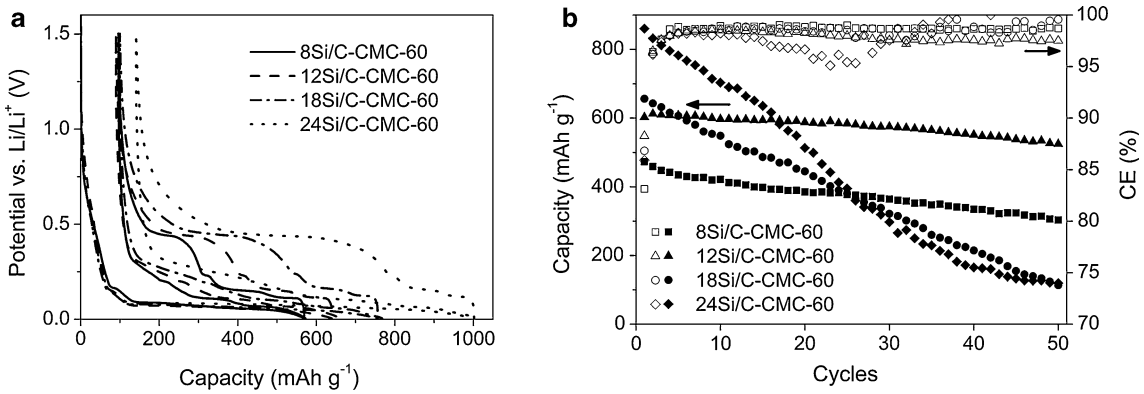

Fig. 7 Potential profiles of the first discharge/charge cycle (**a**) and cyclability (**b**) of anodes prepared by using the CMC binder and Si/C composites of various silicon contents. The values are related to the mass of Si/C composite in the anode

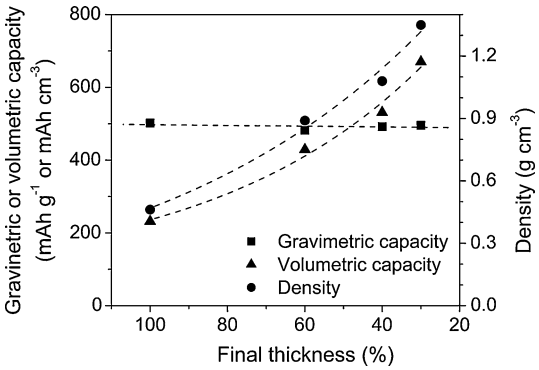

Fig. 8 Evolution of density, first cycle reversible gravimetric capacity, and volumetric capacity of films from the 12Si/C composite and CMC binder press-rolled at different forces. The values are related to the total film mass or volume

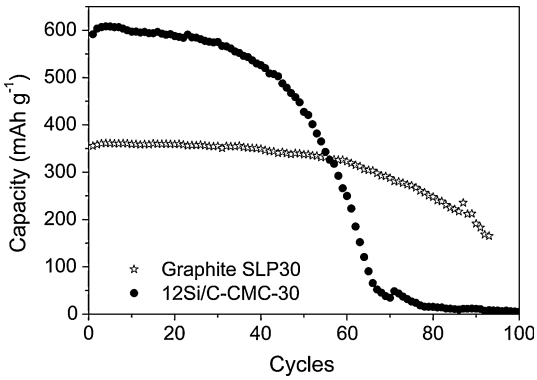

Fig. 10 Cyclability of ~100 μm thick anodes prepared from Si/C composite and commercial battery-grade graphite. The values are related to the mass of active material in the anode

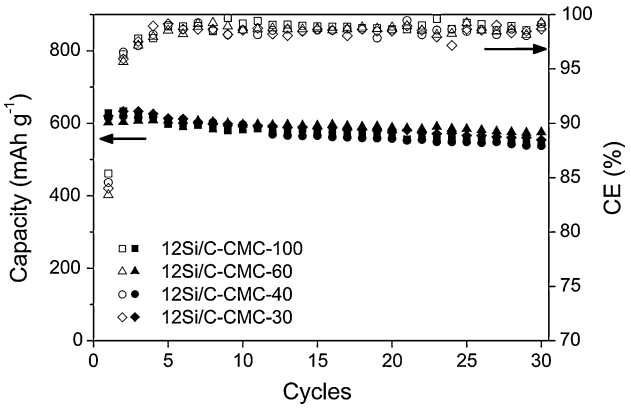

Fig. 9 Cyclability of anodic films prepared from the 12Si/C composite and CMC binder and press-rolled at different forces. The values are related to the mass of Si/C composite in the anode

3.2.4 A long-term cycling in half-cell

The long-term performance of anodes made of the composite 12Si/C-CMC-30 and pure SLP30 graphite was compared in 100 cycle test for ~100 μm thick electrodes (Fig. 10). From the beginning, the composite anode shows somewhat worst performance than the thinner one (Fig. 9); however, a drastic capacity fall is observed after about 40 cycles. In case of graphite-based anode, the decay starts above 60 charge/discharge cycles and proceeds less steeply.

A visual examination of worked-out cells suggests that the performance loss is rather caused by structural defects in the lithium counter electrode than in the anode. After 100 cycles a plastic, metallic lithium (Fig. 11a) changes to the black, amorphous solid (Fig. 11b) which is pyrophoric in air. Such behavior is attributed to the dendrite formation on Li electrode, resulting in internal short circuit to anode via metallic bridges [32, 33]. The parasitic charge flow induces drastic decrease in the capacity measured. As the effect is proportional to absolute charge swing during single charge/discharge cycle, a faster cell failure is observed in the case of Si/C-based anode. The study shows that cycling in half-cell is unsuitable for the evaluation of long-term performance of anode. Full-cell durability tests with commercial cathode are planned for near future.

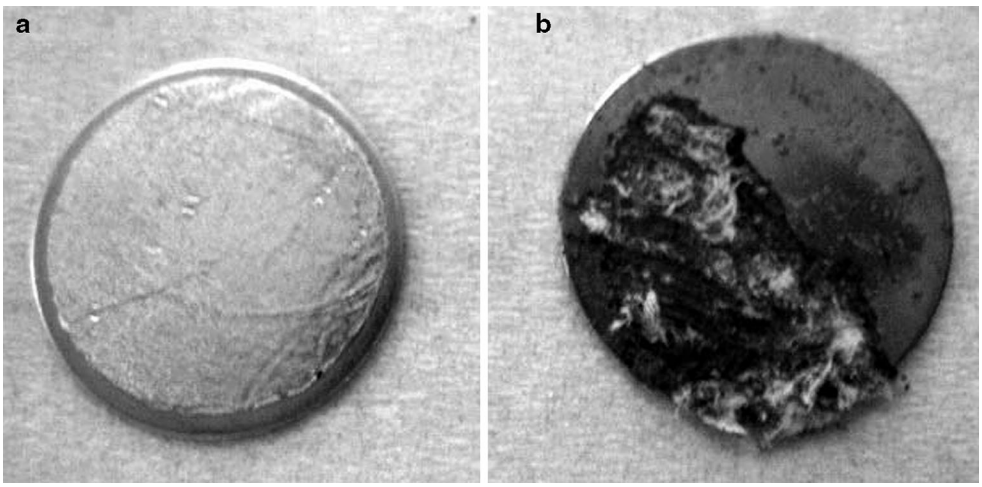

Fig. 11 The morphology of metalic lithium on stainless steel plate used as counter electrode in CR2032-type half-cell: **a** before cell assembling, **b** after 100 cycles of charge/discharge. *White fibers* on the image come from separator

4 Conclusions

A facile and easily scalable synthesis procedure of silicon/carbon composites from cheap and commonly used parent materials has been presented. Milling micro-sized silicon in a toluene-pitch suspension followed by mixing with battery-grade graphite and heat-treating at 1,100 °C leads to an active material composed of silicon and graphite microparticles embedded in a conductive pitch-based carbon matrix. A relatively low irreversible capacity of the anode, below 100 mAh g^{-1}, could be achieved, thanks to a specific structure and morphology of the composite, as well as to a minimized contribution of the CMC binder and percolator, down to 20 wt%. The best performance, corresponding to a reasonable cyclability, coulombic efficiency of about 0.3 %, and a high reversible capacity of 620 mAh g^{-1} was measured for the composite with 12 wt% of silicon. Applying an intensive press-rolling of the composite-based anodic mass enhances the packing density to 1.35 g cm^{-3} without reducing the capacity and worsening the mechanical properties of the film. Volumetric capacity of the resultant film exceeds that of industrial graphite anodes by about 10 %. To keep acceptable cycle performance, the anode thickness should not exceed 80 μm. A further improvement in the performance seems to be possible by optimizing the silicon content in the composite together with limiting the anode work potential window. Such tests should be done in full-cell system with various cathode/anode ratio to avoid the contribution from metallic lithium cathode decay during long-term cycling in half-cell on system performance.

Acknowledgments The research was supported by the Wrocław Research Centre EIT+ within the project "The Application of Nanotechnology in Advanced Materials"—NanoMat (POIG.01.01.02-02-002/08) cofinanced from the resources of European Fund of Regional Development (PO IG 1.1.2).

References

1. Endo M, Kim YJ, Park KC (2010) Advanced battery applications of carbons. In: Beguin F, Frackowiak E (eds) Carbons for electrochemical energy storage and conversion systems. CRC Press, London, pp 469–507
2. Novak P, Goers D, Spahr ME (2010) Carbon materials in lithium-ion batteries. In: Beguin F, Frackowiak E (eds) Carbons for electrochemical energy storage and conversion systems. CRC Press, London, pp 263–328
3. Ishii Y, Fujita A, Nishida T, Yamada K (2001) High-performance anode material for lithium-ion rechargeable battery. Hitachi Chem Tech Rep 36:27–32
4. Zheng T, Dahn JR (1999) Application of carbon in lithium-ion batteries. In: Burchell TD (ed) Carbon materials for advanced technologies. Pergamon, Amsterdam, pp 341–387
5. Yoshio M, Tsumura T, Dimov N (2005) Electrochemical behaviors of silicon based anode material. J Power Sources 146:10–14
6. Wang GX, Ahn JH, Yao J, Bewlay S, Liu HK (2004) Nanostructured Si-C composite anodes for lithium-ion batteries. Electrochem Commun 6:689–692
7. Chan CK, Peng H, Liu G, McIlwrath K, Zhang XF, Huggins RA, Cui Y (2008) High-performance lithium battery anodes using silicon nanowires. Nat Nanotechnol 3:31–35
8. Miyaki Y (2005) US Patent, Patent No: US 6,908,709 B2
9. Foster D, Wolfenstine J, Read J, Allen JL (2008) Performance of Sony's alloy based Li-ion battery. Army Research Laboratory, ARL-TN-0319
10. Xing W, Wilson AM, Eguchi K, Zank G, Dahn JR (1997) Pyrolyzed polysiloxanes for use as anode materials in lithium-ion batteries. J Electrochem Soc 144:2410–2416
11. Liu Y, Hanai K, Yang J, Imanishi N, Hirano A, Takeda Y (2004) Silicon/carbon composites as anode materials for Li-ion batteries. Electrochem Solid-State Lett 7:A369–A372

12. Liu WR, Wang JH, Wu HC, Shieh DT, Yang MH, Wu NL (2005) Electrochemical characterizations on Si and C-coated Si particle electrodes for lithium-ion batteries. J Electrochem Soc 152:A1719–A1725
13. Holzapfel M, Buqa H, Krumelch F, Novak P, Petrat FM, Velt C (2005) Chemical vapor deposited silicon/graphite compound material as negative electrode for lithium-ion batteries. Electrochem Solid-State Lett 8:A516–A520
14. Dimov N, Kugino S, Yoshio M (2004) Mixed silicon-graphite composites as anode material for lithium ion batteries—influence of preparation conditions on the properties of the material. J Power Sources 136:108–114
15. Zhang Z, Wang Y, Ren W, Tan Q, Chen Y, Li H, Zhong Z, Su F (2014) Scalable synthesis of interconnected porous silicon/carbon composites by the Rochow reaction as high-performance anodes of lithium ion batteries. Angew Chem Int Edit 53:5165–5169
16. Yu J, Zhan H, Wang Y, Zhang Z, Chen H, Li H, Zhong Z, Su F (2013) Graphite microspheres decorated with Si particles derived from waste solid of organosilane industry as high capacity anodes for Li-ion batteries. J Power Sources 228:112–119
17. Eker Y, Kierzek K, Raymundo-Pinero E, Machnikowski J, Beguin F (2010) Effect of electrochemical conditions on the performance worsening of Si/C composite anodes for lithium batteries. Electrochim Acta 55:729–736
18. Wang YX, Chou SL, Kim JH, Liu HK, Dou SX (2013) Nanocomposites of silicon and carbon derived from coal tar pitch: cheap anode materials for lithium-ion batteries with long cycle life and enhanced capacity. Electrochim Acta 93:213–221
19. Bridel JS, Azaïs T, Morcrette M, Tarascon JM, Larcher D (2010) Key parameters governing the reversibility of Si/carbon/CMC electrodes for Li-ion batteries. Chem Mater 22:1229–1241
20. Komaba S, Shimomura K, Yabuuchi N, Ozeki T, Yui H, Konno K (2011) Study on polymer binders for high-capacity SiO negative electrode of Li-ion batteries. J Phys Chem C 115:13487–13495
21. Li J, Lewis RB, Dahn JR (2007) Sodium arcboxymethyl cellulose: a potential binder for Si negative electrodes for Li-ion batteries. Electrochem Solid-State Lett 10:A17–A20
22. Magasinski A, Zdyrko B, Kovalenko I, Hertzberg B, Burtovyy R, Huebner CF, Fuller TF, Luzinov I, Yushin G (2010) Toward efficient binders for Li-ion battery Si-based anodes: polyacrylic acid. Appl Mater Interfaces 2:3004–3010
23. Datta MK, Kumta PN (2007) Silicon, graphite and resin based hard carbon nanocomposite anodes for lithium ion batteries. J Power Sources 165:368–378
24. Choi H, Lee W, Kim DU, Kumar S, Kim SS, Chung HS, Kim JH, Ahn YC (2010) Effect of grinding aids on the grinding energy consumed during grinding of calcite in a stirred ball mill. Miner Eng 23:54–57
25. Dubinin MM (1989) Fundamentals of the theory of adsorption in micropores of carbon adsorbents: characteristics of their adsorption properties and microporous structures. Carbon 27:457–467
26. Stoeckli F, López-Ramón MV, Hugi-Cleary D, Guillot A (2001) Micropore sizes in activated carbons determined from the Dubinin–Radushkevich equation. Carbon 39:1115–1116
27. Lee JH, Kim WJ, Kim JY, Lim SH, Lee SM (2008) Spherical silicon/graphite/carbon composites as anode material for lithium-ion batteries. J Power Sources 176:353–358
28. Obrovac MN, Krause LJ (2007) Reversible cycling of crystalline silicon powder. J Electrochem Soc 154:A103–A108
29. Zhang Z, Zeng T, Lai Y, Jia M, Li J (2014) A comparative study of different binders and their effects on electrochemical properties of $LiMn_2O_4$ cathode in lithium ion batteries. J Power Sources 247:1–8
30. Dimov N, Xia Y, Yoshio M (2007) Practical silicon-based composite anodes for lithium-ion batteries: fundamental and technological features. J Power Sources 171:886–893
31. Ishii Y, Nishida T, Suda T, Kobayashi M (2006) Anode material for high energy density rechargeable lithium-ion battery. Hitachi Chem Tech Rep 47:29–32
32. Ota M, Izuo S, Nishikawa K, Fukunaka Y, Kusaka E, Ishii R, Selman JR (2003) Measurement of concentration boundary layer thickness development during lithium electrodeposition onto a lithium metal cathode in propylene carbonate. J Electroanal Chem 559:175–183
33. Rosso M, Brissot C, Teyssot A, Dollé M, Sannier L, Tarascon JM, Bouchet R (2006) Dendrite short-circuit and fuse effect on Li/polymer/Li cells. Electrochim Acta 51:5334–5340